Available online at www.sciencedirect.com

SCIENCE DIRECT

Biochimica et Biophysica Acta 1716 (2005) 137 – 145

BIOCHIMICA ET BIOPHYSICA ACTA BBA

http://www.elsevier.com/locate/bba

Membrane-bound peptides mimicking transmembrane Vph1p helix 7 of yeast V-ATPase: A spectroscopic and polarity mismatch study

Renske W. Hesselink, Rob B.M. Koehorst, Petr V. Nazarov, Marcus A. Hemminga *

Laboratory of Biophysics, Wageningen University, Dreijenlaan 3, NL-6703 HA, P.O. Box 8128, 6700 ET Wageningen, The Netherlands

Received 12 July 2005; received in revised form 29 August 2005; accepted 30 August 2005
Available online 16 September 2005

Abstract

The V-ATPases are a family of ATP-dependent proton pumps, involved in a variety of cellular processes, including bone breakdown. V-ATPase enzymes that are too active in the latter process can result in osteoporosis, and inhibitors of the enzyme could be used to treat this disease. As a first step in studying the structure and function of the membrane-embedded interface at which proton translocation takes place, and its role in V-ATPase inhibition, synthetic peptides P1 and P2 consisting of 25 amino acid residues are presented here that mimic Vph1p helix 7 of yeast V-ATPase. A single mutation R10A between peptide P1 and P2 makes it possible to focus on the role of the essential arginine residue R735 in proton translocation. In the present work, we use a novel combination of spectroscopic techniques, such as CD spectroscopy, tryptophan emission spectra, acrylamide quenching and parallax analysis, and polarity mismatch modeling to characterize the peptides P1 and P2 in lipid bilayer systems. Based on both the spectroscopic experiments and the polarity mismatch modeling, P1 and P2 adopt a similar transmembrane conformation, with a mainly α-helical structure in the central part, placing the tryptophan residue at position 12 at a location 4±2 Å from the centre of the lipid bilayer. Furthermore, the arginine at position 10 in P1 does not have an effect on the bilayer topology of the peptide, showing that the long, flexible side chain of this residue is able to snorkel towards the lipid headgroup region. This large flexibility of R735 might be important for its function in proton translocation in the V-ATPase enzyme.

Keywords: V-ATPase; Transmembrane peptide; Protein–lipid interaction; Arginine snorkeling; Tryptophan location; Polarity mismatch simulation

1. Introduction

The vacuolar H^+-ATPases, or V-ATPases, are a family of proton pumps, which hydrolyze ATP and use the released energy to pump protons across a membrane [1–3]. In most cases this membrane surrounds an organelle in the cell, such as a vacuole, endosome, or lysosome. The V-ATPase acidifies these compartments, which is important for a variety of cellular processes, including ligand–receptor dissociation, targeting of enzymes and transport of small molecules. In certain cases, V-ATPases can also be found in the cell membrane, where they function in acidification of the extracellular space. This is for example the case in osteoclasts, cells that break down bone tissue by acidifying a small volume next to the bone [4]. When the V-ATPase enzymes in osteoclasts are too active, bone breakdown can exceed bone formation by osteoblasts, and a disease known as osteoporosis develops. Selective and potent inhibitors of the V-ATPase could be used to treat this disease; this is one of the reasons why studying the structure, function, and inhibitor binding sites of the V-ATPase is important [5].

The V-ATPases structurally resemble the F-ATPases, which catalyze the opposite reaction: synthesis of ATP using the energy from a proton gradient. The F-ATPases have been studied extensively, and the resemblance has been useful in building a structural and functional model of the V-ATPase [1–3]. Recently, the structure at 2.1 Å resolution of the membrane rotor ring from the vacuolar-type (V-type) sodium

Abbreviations: 5-DOX-PC, 1-Palmitoyl-2-stearoyl(5-DOXYL)-*sn*-glycero-3-phosphocholine; 12-DOX-PC, 1-Palmitoyl-2-stearoyl(12-DOXYL)-*sn*-glycero-3-phosphocholine; CD, Circular dichroism; DOPC, 1,2-Dioleoyl-*sn*-glycero-3-phosphocholine; DOPG, 1,2-Dioleoyl-*sn*-glycero-3-[phospho-rac-(1-glycerol)]; K_{SV}, Stern–Volmer constant; *L*/*P*, Lipid to peptide molar ratio; LUV, Large unilamellar vesicle; TEMPO-PC, 1,2-Dioleoyl-*sn*-glycero-3-TEMPO-phosphocholine; TFE, Trifluoroethanol; V-ATPase, Vacuolar H^+-ATPase enzyme

* Corresponding author. Tel.: +31 317 482635/+31 317 482044; fax: +31 317 482725.
E-mail address: marcus.hemminga@wur.nl (M.A. Hemminga).

0005-2736/$ - see front matter © 2005 Elsevier B.V. All rights reserved.
doi:10.1016/j.bbamem.2005.08.010

ion-pumping adenosine triphosphatase (Na^+-ATPase) from *Enterococcus hirae* was obtained [6]. The subunits in this ring are homologs of the 16-kDa and 8-kDa proteolipids found in other V-ATPases and in F-ATPases, respectively. The V-ATPase enzyme of yeast consists of two domains: the cytoplasmic, water-soluble V_1 domain, at which ATP-hydrolysis takes place, and the membrane-bound V_0 domain. The latter domain comprises a core formed by a hexameric complex of the three different proteolipid subunits Vma3p (4×), Vma11p (1×), and Vma16p (1×), which is in contact with a transmembrane element of Vph1p. Interaction between a glutamate (E137) in the putative transmembrane helix 4 of the proteolipid subunits and an arginine (R735) in the putative transmembrane helix 7 of Vph1p are found to be essential for proton translocation [7].

The V-ATPases are thought to operate via a mechanism, in which rotation of the hexameric ring of Vma3p, Vma11p, and Vma16p relative to Vph1p drives unidirectional proton transport [3]. Vph1p [8] and Vma3p [9–12] in V-ATPase, as well as the interface between the corresponding subunits in the related F-ATPase [13] are shown to bind bafilomycin and concanamycin, which are well-known inhibitors of these enzymes.

Synthetic peptides that resemble trans-membrane sections of membrane proteins are suitable model systems for biophysical studies to obtain insight in the molecular interactions that play a role in the native system [14–18]. This approach is justified by the two-stage model of membrane protein folding, which suggests that trans-membrane helices are independently stable in lipid bilayers. Studying a single helix may thus provide insight into the more complex membrane protein [19–21].

The amino acid sequence of the peptides, hydrophobic matching, and interfacial anchoring determine the interactions of the peptides with the lipid bilayer, and with other membrane-inserted peptides, and hence their bilayer topology [22–27]. Although hydrophobic residues tend to predominate in transmembrane helices, polar and ionisable residues are particularly important in determining helix behavior. The ability of such residues to form hydrogen bonds or salt bridges often promotes helix–helix interactions [28–33], similar as would be expected for those between Vph1p helix 7 and Vma3p helix 4. Single transmembrane helices can also contain polar or ionisable residues, although the introduction of too many hydrophilic residues can result in the formation of shifted or non-transmembrane states [34,35]. Residues having a longer side chain, such as lysines or arginines, can be buried in the bilayer core more easily because they can position their charged group near the lipid headgroups by snorkeling towards the lipid/water interface [15,35–38].

As a first step in studying the structure and function of the membrane-embedded interface between helix 4 of Vma3p and helix 7 of Vph1p, and its role in V-ATPase inhibition, synthetic peptides are presented here that mimic Vph1p helix 7 of yeast V-ATPase [3,7] (see Fig. 1). The designed peptides contain a single Trp residue near the centre of the peptide sequence that enables the study of their physicochemical behavior in lipid bilayer systems by fluorescence spectroscopy. A single mutation R10A between peptide P1 and P2 makes it possible to focus on the role of R735 in the complex formation and proton translocation of the V-ATPase. Both peptides have two lysines added on the C and N-terminal ends that serve as membrane anchors and improve the solubility of the peptides [24,39].

IHTIEFCLNCV<u>SHTASYLRLWALSLAHAQLSS</u>VLWTM

TM7

KKSHTASYL**R**LWALSLAHAQLSSKK

P1

KKSHTASYL**A**LWALSLAHAQLSSKK

P2

Fig. 1. Primary sequence of transmembrane helix 7 (TM7) of subunit a (Vph1p) of yeast V-ATPase [40], and the chemically synthesized peptides, P1 and P2, used in this work. In TM7, the chemically synthesized region is underlined. P1 contains 21 amino acid residues of TM7, with two lysines added on the C and N-terminal ends of the peptide to facilitate reconstitution into bilayers. P2 has the same sequence as P1, except for the mutation R10A. The amino acid residues involved in this mutation are underlined and indicated in bold.

In the present work, we use a novel combination of spectroscopic techniques and polarity mismatch modeling to characterize the peptides P1 and P2 in lipid bilayer systems. Comparison of the behavior of P1 and P2 allows us to specifically study the role of the arginine residue R735 in the determination of the bilayer topology of the peptides, and to extend this to its role in the native system.

2. Materials and methods

2.1. Chemicals

1,2-Dioleoyl-*sn*-glycero-3-phosphocholine (DOPC; $(18:1)_2$-PC) was purchased from Sigma and 1,2-dioleoyl-*sn*-glycero-3-[phospho-*rac*-(1-glycerol)] (DOPG; $(18:1)_2$-PG) was purchased from Avanti Polar Lipids Inc. Spin-labeled lipids 1,2-dioleoyl-*sn*-glycero-3-phospho(TEMPO)choline (TEMPO-PC), 1-palmitoyl-2-stearoyl-(5-DOXYL)-*sn*-glycero-3-phosphocholine (5-DOX-PC) and 1-palmitoyl-2-stearoyl-(12-DOXYL)-*sn*-glycero-3-phosphocholine (12-DOX-PC) were purchased from Avanti Polar Lipids Inc. All other chemicals and solvents were purchased from Merck, except for TFE, which was from Acros organics.

2.2. Peptide synthesis and design

The peptides P1 and P2 (see Fig. 1) were produced on solid support using continuous flow chemistry by Pepceuticals Ltd., Leicester, UK and used without further purification. The final purity was tested by HPLC and mass spectrometry, and was above 90% in all cases. Peptide P1 contains 21 residues from the native sequence [40] of trans-membrane helix 7 of yeast V-ATPase Vph1p, which has recently been established to run from residues V727 to T752 [2,3,7]. Arginine R735 in the native sequence [40] corresponds to R10 in the peptide. This arginine has shown to be essential for proton translocation of the V-ATPase [7].

On both sides of the peptide, two lysines are added. This approach is frequently used in studies of membrane-bound peptides, as lysines are known to increase solubility, stabilize membrane insertion by interaction with anionic lipid headgroups, promote a trans-membrane configuration and minimize aggregation [24,27,41]. The arginine residue in peptide P1 is the only residue that is essential for proton transport activity in the native enzyme. To study its role in more detail, a second peptide (P2) is designed, with the single substitution R10A. In both peptides, the centrally located tryptophan residue W12 acts as a fluorescence reporter group.

Phospholipid model systems represent a suitable model environment for the peptides. It may be that in the V-ATPase complex helix 7 is not exposed to lipids, however, phospholipid bilayers provide the best possible polarity gradient from an apolar to a polar medium to incorporate this protein domain for our biophysical work [24,27,41].

2.3. Vesicle preparation

Desired amounts of lipids (DOPC and DOPG in 4:1 mole ratio, further denoted as DOPC/DOPG) in chloroform and peptides in methanol (P1) or TFE (P2), were mixed and dried under a stream of nitrogen. Traces of solvent were removed by further evaporation over night under vacuum. Buffer (10 mM NaH_2PO_4/Na_2HPO_4, pH=7.0) was added to the dried samples, and three cycles of vortexing, freezing, and thawing were carried out to obtain crude multilamellar vesicles. The large unilamellar vesicles (LUVs) used in this study were prepared by extrusion, using filters with 100 nm pore size. Although small unilamellar vesicles (SUVs) would have a lower light scattering having less interference with our optical experiments, they are known to produce anomalous peptide binding, resulting perhaps from distorted lipid packing associated with the high surface curvature. On the contrary, LUVs have larger radii of curvature and are therefore more suitable models of biological membranes; for that reason, LUVs are used in the present work [42].

2.4. CD measurements

CD spectra were recorded using a Jasco spectropolarimeter J-715. The samples contained 1 mM of lipid and 18 μM of peptide (L/P=55) and were measured in a cuvette with 1 mm pathlength. Spectra were recorded between 190 and 260 nm using the following parameters: scan speed 50 nm min^{-1}, data pitch 0.5 nm, 2 s response time, 1 nm bandwidth. Forty spectra were accumulated and the background signal was subtracted. The spectra were analyzed using the freeware program CDNN 2.1 [43].

2.5. Absorption and fluorescence measurements

Absorption measurements were carried out on a Cary 5E (Varian) spectrophotometer. Absorption spectra were recorded to determine peptide concentrations, using the well-known extinction coefficients of tryptophan and tyrosine [44], and to correct for inner filter effects in our fluorescence experiments. Fluorescence spectra were recorded on a Fluorolog 3.22 (Jobin Yvon-Spex), using 1 ml quartz cuvettes with pathlengths of 10 and 4 mm in the excitation and emission direction, respectively. Fluorescence spectra were recorded between 300 and 500 nm, using an excitation wavelength of 290 nm and using excitation and emission slits giving a 2-nm bandpass. Spectra were corrected for wavelength dependent variations in the detection, and for background fluorescence. To correct for the inner filter effect Eq. (1) was used [45]:

$$F_{corr} = F_{obs} 10^{(l_{ex}A_{ex}+l_{em}A_{em})/2}. \quad (1)$$

Here, F_{obs} and F_{corr} are the observed and the corrected fluorescence intensities, respectively. A_{ex} and A_{em} are the absorbances at the excitation and emission wavelengths, respectively. l_{ex} and l_{em} are the lengths in cm of the optical paths of excitation and emission, respectively. For the fluorescence measurements, the lipid concentration was 200 μM and the peptide concentration 2 μM (L/P=100). In all cases, the background signal was at most 10% of the total signal.

2.6. Quenching experiments

For acrylamide quenching experiments, 5 μl aliquots of a 3 M stock solution were added to 1 ml samples, until a final concentration of 0.12 M acrylamide was reached. The fluorescence intensity was measured after each addition. Measurements were repeated until there was no decrease in intensity to any further extent. The fluorescence intensity was corrected for the dilution by the acrylamide solution. Quenching of a homogeneous population of fluorophores, either via a collisional or via a static process, follows the Stern–Volmer equation [45]:

$$\frac{F_0}{F} = 1 + K_{SV}[Q]. \quad (2)$$

In this equation, F_0 and F are the fluorescence intensities in the absence and presence of quencher, respectively. [Q] is the quencher concentration and K_{SV} the Stern–Volmer constant. K_{SV} provides information on the accessibility of the fluorophores to the quencher [45].

2.7. Parallax analysis

In a so-called parallax analysis the extent of quenching by lipids labeled with a doxyl group at different depths is compared, and the distance of the tryptophan residue to the centre of the bilayer is calculated from these quenching efficiencies [46]. In this study, the amount of quenching by PC lipids with a spin-label linked to the headgroup or to the hydrocarbon chain at C-atom number 5 or 12 (TEMPO-PC, 5-DOX-PC, and 12-DOX-PC, respectively) is compared. For this purpose 12.5 mol% of DOPC was replaced by spin-labeled lipid. This gives a final concentration of 10 mol% spin-labeled lipid in the samples. The decrease in fluorescence intensity in the samples with TEMPO, 5-DOX, or 12-DOX-PC compared to the sample without spin-labeled lipid gives an indication of the position of the tryptophan residue. Only the data from the latter two were used to calculate the depth of the tryptophan residue in the bilayer.

The decrease in fluorescence intensity in the samples with 5 or 12-DOX-PC compared to the sample without spin-labeled lipid was used to calculate the depth of the tryptophan residue in the bilayer. For the calculation of the Trp to bilayer centre distance (z_{cf}), taking into account quenching by the deep quencher from both leaflets of the lipid bilayer, the following modified version of the parallax equation was used [23]:

$$z_{cf} = L_{c2} - \left[\left(\frac{1}{\pi C}\ln\left\{\left(\frac{F_1}{F_0}\right)^2 \Big/ \frac{F_2}{F_0}\right\} - 2L_{21}^2 + 4L_{c2}^2\right) \Big/ 4(L_{21}+L_{c2})\right] \quad (3)$$

In this equation L_{c2} is the difference in depth between the deep quencher (12-DOX-PC) and the bilayer centre, L_{21} is the difference in depth between the shallow (5-DOX-PC) and the deep (12-DOX-PC) quencher and C is the concentration of the quencher in molecules per $Å^2$. F_0, F_1, and F_2 are the fluorescence intensities in the absence of quencher, and in the presence of 5-DOX-PC and 12-DOX-PC, respectively.

2.8. ESR measurements

Samples containing spin-labeled lipid were checked by ESR measurements to ensure that all samples contained equal amounts of unpaired electrons (quenchers). First derivative absorption ESR spectra were measured at room temperature on an X-band Bruker ESP 300 E spectrometer. The sweep width of the recorded spectra was 20 mT, the microwave power was 10 mW, the field frequency was 9.33 GHz, and the centre of the field was 0.333 T. The samples were contained in 200 μl capillaries. Only small differences were found between the samples, for which corrections were made in the calculations.

3. Results

3.1. CD spectroscopy

In Fig. 2, the CD spectra of P2 in buffer and reconstituted into DOPC/DOPG vesicles are presented. The result for P1 is identical (data not shown). The spectrum of the peptide in buffer indicates a predominantly unordered conformation with low helix content. The spectrum of the reconstituted peptide on the other hand, has a higher intensity and shows minima at 208 and 222 nm, characteristic for an α-helix conformation.

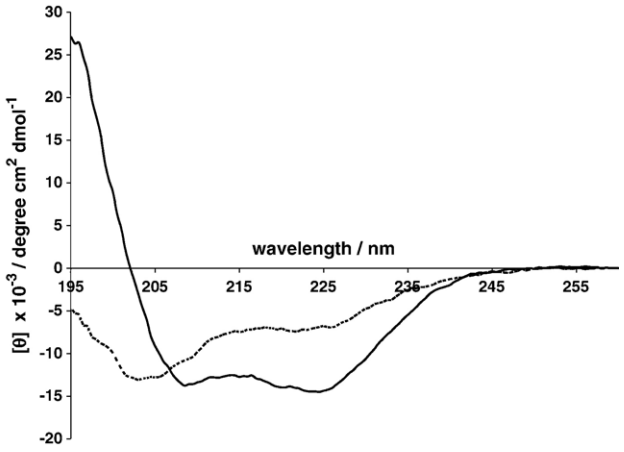

Fig. 2. CD spectra of P2 in buffer (dashed line) and reconstituted into DOPC/DOPG vesicles (solid line). In buffer the peptide is predominantly unstructured with an α-helical content of ~15%, while in vesicles the peptide has more structure with a helicity of ~45%.

The difference between the water-dissolved and membrane-bound conformation is confirmed by quantitative analysis using the program CDNN 2.1. In buffer, the peptide has a helix content of 15±5%, the remainder being mainly random coil (40%). For the vesicle-bound form, the helix content is 45±5%, while the percentage random coil has decreased to about 25–30%. The error values are due to uncertainties in peptide concentration.

3.2. Fluorescence spectra

The fluorescence spectra of P1 and P2 in buffer (see Fig. 3) resemble that of the earlier reported class III tryptophan fluorescence spectrum [47] and nearly coincide with that of free tryptophan in water. This indicates that at low peptide concentrations the peptides are soluble in water and do not tend to aggregate; aggregation would place the tryptophan residue in a more hydrophobic peptide environment, and thereby shift the fluorescence maximum to the blue. Fig. 3 also shows the fluorescence spectra of P1 and P2 reconstituted into DOPC/DOPG vesicles. The fluorescence maxima of P1 and P2 in vesicles are 330 and 329 nm, respectively, giving a blue shift of approximately 20 nm as compared to the maxima found for the peptides in buffer. In our studies with varying *L*/*P* ratio, the fluorescence spectra were already completely blue-shifted at the lowest lipid concentration, and did not shift anymore at higher lipid concentrations. This is a strong indication for complete membrane association of the peptides at all *L*/*P* ratios.

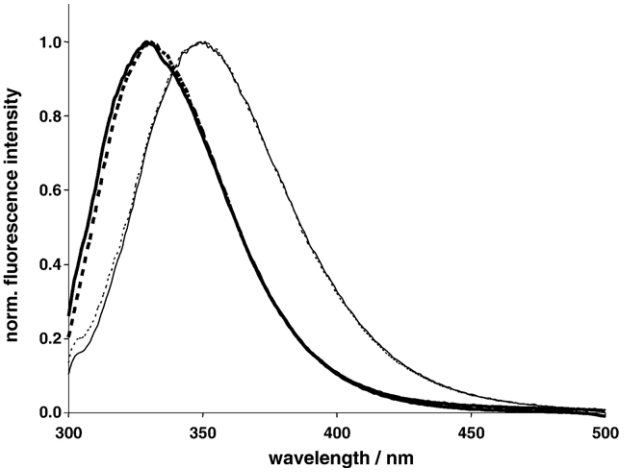

Fig. 3. Normalized fluorescence spectra of P1 (dashed line) and P2 (solid line) in buffer (thin lines) and reconstituted into DOPC/DOPG vesicles (thick lines).

3.3. Acrylamide quenching

In Fig. 4, the Stern–Volmer plot for acrylamide quenching of P1 and P2 reconstituted in DOPC/DOPG vesicles is shown. For comparison Stern–Volmer plots for completely accessible free tryptophan in water [45] and for tryptophan completely buried in a membrane [14,22,48] are included.

3.4. Parallax analysis

In Fig. 5a, fluorescence spectra are presented for P2 in DOPC/DOPG vesicles in the absence and presence of spin-labeled lipids. The spectra show a decreasing quenching efficiency in the order: 12-DOX-PC > 5-DOX-PC > TEMPO-PC. To observe possible quencher-induced shifts, the normalized fluorescence spectra for P2 in vesicles in the absence and presence of either 5-DOX-PC or 12-DOX-PC are presented in Fig. 5b. The results for P1 are similar (not shown here). In this figure, it can be seen that although the line shapes show a small

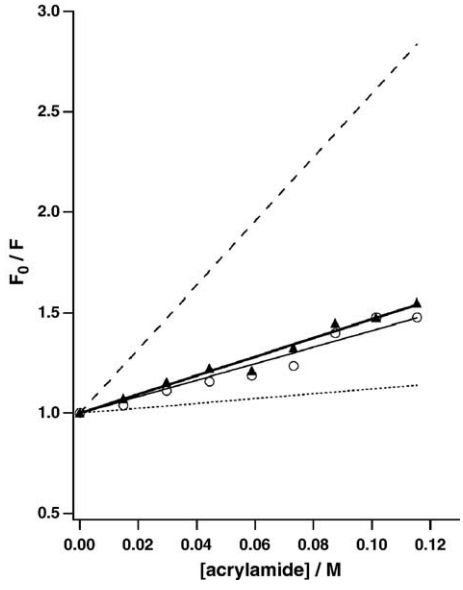

Fig. 4. Stern–Volmer plots for acrylamide quenching of P1 (▲) and P2 (○) in vesicles with their fits (thick and thin solid line, respectively) according to Eq. (2). Theoretical lines for completely shielded (dotted line; K_{SV}=1.2 M^{-1} [14,22,48]) and completely exposed tryptophan (dashed line; K_{SV}=16 M^{-1} [45]) are included for comparison.

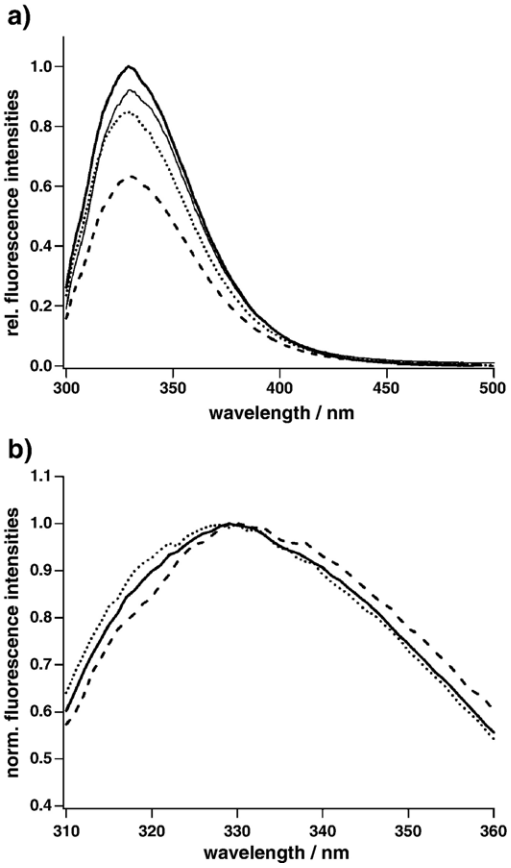

Fig. 5. (a) Fluorescence spectra of P2 in DOPC/DOPG vesicles containing 10% TEMPO-PC (thin solid line), 5-DOX-PC (dotted line), or 12-DOX-PC (dashed line), having intensities normalized to that without quencher (thick solid line); (b) Normalized fluorescence spectra of P2 in DOPC/DOPG vesicles, showing small shifts of the fluorescence maximum upon addition of 5-DOX-PC (dotted line), and 12-DOX-PC (dashed line), with respect that with no quencher (solid line).

difference, the wavelength of maximum intensity (λ_{max}) does hardly change.

4. Discussion

In this study, we have presented model peptides (P1 and P2) for helix 7 of Vph1p of the V-ATPase enzyme. Peptide P1 contains a specific arginine R735 from the V-ATPase, which is essential for proton translocation by this enzyme. In peptide P2, the arginine is mutated into an alanine to enable to examine the role of the arginine in the enzyme. By using CD spectroscopy and different fluorescence techniques, including tryptophan emission spectra, quenching by acrylamide and parallax analysis, the behavior of the peptides in phospholipid vesicles is characterized.

4.1. CD spectra

Qualitative as well as quantitative analysis of the CD spectra shown in Fig. 2 demonstrate that both peptides P1 and P2 are mainly unstructured in buffer, while they adopt a ~45% α-helical conformation in vesicles. The shape of the CD spectrum in vesicles is very similar to the shape of a perfect α-helix, however, the intensity is reduced. We interpret this observation as arising from motional dynamics of the peptide backbone. The small α-helical peptides P1 and P2 are expected to be relatively flexible systems undergoing rapid equilibria among multiple conformational states. This means that longer helices would break up in smaller domains in a dynamic way. From theoretical CD studies it is known that α-helices with a smaller length give rise to a lower CD intensity [49]. Most probably, the C and N-terminal ends of the peptide sequence, consisting of positively charged lysines and some other polar residues, form a non-helical structure to interact as favorably as possible with the negatively charged phospholipid headgroups. Therefore, it follows that the more hydrophobic core of the peptides, including the arginine at position 10 for peptide P1, most likely forms an α-helical structure.

4.2. Fluorescence spectra

The maxima of the tryptophan fluorescence of P1 and P2 in DOPC/DOPG vesicles (~330 nm, see Fig. 3) fall well within the range of values (315 to 344 nm) found for tryptophan residues in the apolar centre of a membrane [14,22–25,48]. As compared to the lowest reported values, the fluorescence maximum is somewhat red shifted, suggesting a position of the tryptophan residue slightly off the centre of the membrane. However, in the case of an α-helical peptide conformation, the red shift could also result from tryptophan forming a hydrogen bond with the tyrosine [47], which is located at the fourth position from the tryptophan.

It is striking to note that there is a strong resemblance between the fluorescence properties of P1 and P2 after reconstitution. This suggests a minor contribution of the strongly hydrophilic arginine at position 10 to the bilayer topology of peptide P1, in agreement with the CD results.

4.3. Acrylamide quenching

From the Stern–Volmer plots presented in Fig. 4, the Stern–Volmer constants (K_{SV}) were calculated for P1 and P2 in vesicles according to Eq. (2). For both peptides the K_{SV} values amount to a value of $4.4 \pm 0.4\ M^{-1}$. This value is in between the K_{SV} for completely water-accessible ($K_{SV}=16\ M^{-1}$) [45] and completely shielded ($K_{SV}=1.2\ M^{-1}$) tryptophan [14,22,48], indicating that for both peptides the tryptophan residue is buried to some extent into the membrane, being still slightly accessible to acrylamide. The Stern–Volmer plots do not show a deviation from linearity. This is indicative for a high population homogeneity [45] and suggests the existence of only a transmembrane population of the peptides in DOPC/DOPG vesicles, consequently having their tryptophan residues close to the centre of the membrane. The observed blue shift of the fluorescence maximum of the peptides in vesicles as compared to that in buffer is in agreement with this finding. Furthermore, a transmembrane configuration is supported by fluorescent studies of a peptide similar to P1 in which the arginine at position 10 is replaced by a histidine that has been

examined at neutral pH in bilayers with varying thickness (Hesselink et al., unpublished results).

4.4. Parallax analysis

The fluorescence maxima and acrylamide quenching results only give a first indication of the position of the tryptophan in the centre of the membrane, but not a quantitative value. However, the parallax method allows us to calculate the depth of the tryptophan residue more accurately, leading to a more precise model for the membrane topology of the peptides. Qualitatively, the decreasing order in quenching efficiency 12-DOX-PC > 5-DOX-PC > TEMPO-PC (see Fig. 5a) confirms the location of the tryptophan residue close to the centre of the bilayer. Quantification of the data using Eq. (3), results in distances of the tryptophan residue to the centre of the bilayer of 4.7 and 4.0 ± 1.9 Å for P1 and P2, respectively. The error value arises from the calculated standard deviations from measurements of four independent reconstitutions. The large error value is due to the uncertainty in peptide concentration, which was determined to be approximately 10%.

Quencher-induced shifts of the fluorescence spectrum can reveal possible heterogeneity of the peptide population. In a sample containing a heterogeneous peptide population, with both deep and shallow tryptophan residues, 5-DOX-PC would quench the latter most strongly, inducing a blue shift, while 12-DOX-PC would have the opposite effect. However, in a homogeneous peptide population no large differences between λ_{max} with and without quenchers would be observed, although even for a relatively uniform peptide population small quencher-induced shifts could be expected due to the distribution of peptides around an average depth.

For P1 and P2 quencher-induced shifts of the flanks of the line shape in the expected directions are indeed observed (see Fig. 5b), but these shifts are small (1 to 2 nm) and λ_{max} is practically the same for all spectra. This strongly indicates a homogeneous conformation and bilayer topology of both peptides P1 and P2 [48].

4.5. Simulation of polarity mismatch between peptides and lipid bilayer

Based on the spectroscopic experiments, P1 and P2 appear to adopt a similar α-helical conformation in lipid bilayers, in which the tryptophan residue is placed near the centre of the bilayer. Furthermore, the arginine at position 10 in P1 does not have an effect on the bilayer topology of the peptide. To support the conclusions from our experiments, we have carried out calculations to minimize the polarity mismatch between the peptide and membrane, allowing for all possible orientations and locations of the peptide with respect to the bilayer. Although CD analysis shows that the conformation of the peptides is different in the water phase as compared to the lipid phase, and that the α-helical content in the lipid phase may not be 100% due to motional dynamics, for simplicity, we will assume in our calculations a full α-helix for the peptides under all conditions.

For the mismatch calculations, three spatial parameters were introduced, defining the position and orientation of the peptide in the bilayer. The related parameters are given by the distance d between the centre of mass of the peptide and the membrane centre, the peptide tilt angle θ, i.e., the angle between the peptide helix and the normal to the membrane surface, and the angle of the coaxial rotation of the peptide ω (Fig. 6). In the simulation model, the charge density profile of the bilayer and the polarity scales of the amino acid residues were used [50]. To make the scales applicable for polarity mismatch optimization, their values were normalized to the range 0 to 1, with 0 corresponding to the most hydrophobic amino acid residue. The polarity profile of the bilayer [50] was approximated by the following empirical equation:

$$P(z) = \frac{1}{1 + (z_C/z)^8}. \quad (4)$$

In this equation $P(z)$ is the scaled polarity at distance z from the bilayer centre and z_C is half the thickness of the hydrophobic membrane region (see Fig. 7a).

The hydrophobicity scales for the amino acid residues [50] include the free energies of amino acid residues transfer from water to the bilayer interface and from water to n-octanol. The mean value of the two free energies, scaled to the range [0,1], was taken as the scaled polarity p of an amino acid residue (see Fig. 7b). The total polarity mismatch M for a peptide, consisting of N amino acid residues, is then calculated as follows:

$$M = \sqrt{\sum_{i=l}^{N} (P(z_i) - p_i)^2}. \quad (5)$$

Here, z_i is the distance of the centre of mass of the ith amino acid residue to the bilayer centre and p_i is the polarity of this

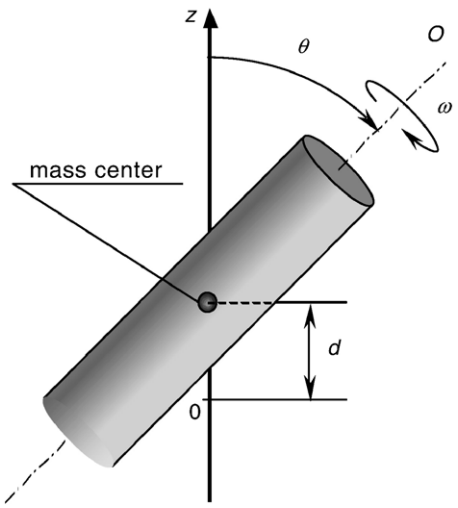

Fig. 6. Model describing the peptide incorporation into the bilayer given by the spatial parameters d, θ, and ω. The center of mass of each amino acid residue was calculated taking into account the coordinates and atomic weights of all peptide atoms. The normal to the membrane plane is shown by the z-axis with $z = 0$ corresponding to the membrane center, the symmetry axis of the peptide by the axis O.

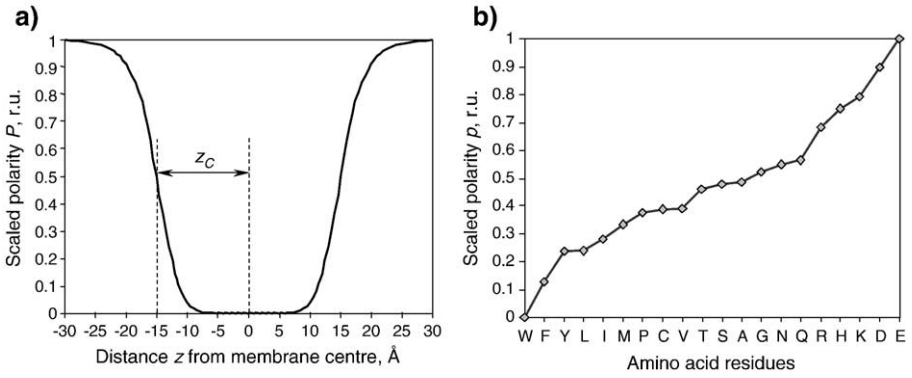

Fig. 7. (a) Scaled polarity profile approximation of a bilayer [50]. The thickness of a single lipid leaflet of the hydrophobic membrane region is given by z_C. (b) Scaled polarity values for different amino acid residues originating from White and Wimley's scale [50].

residue. Obviously, the polarity mismatch M is a function of the orientation (θ, ω) and depth d of the peptide with respect to the membrane. Therefore, the Nelder–Mead optimization algorithm [51] was applied to find the parameters d, θ, and ω corresponding to the state of the peptide with the smallest mismatch. This algorithm provides a reasonable convergence and is not extremely time consuming. It should be noted that we use here a simplified model that is only based on hydrophobic effects. For example, we do not take into account electrostatic effects of the phospholipid headgroups. However, the presence of negatively charged lipid headgroups of DOPG will increase the anchoring of the positively charged lysines and therefore stimulate a transmembrane orientation of the peptides.

Minimizations of the polarity mismatch between the peptides and the membrane were performed 1000 times with different initial estimations of d, θ, and ω to avoid trapping in local minima. The resulting global minimum for the mismatch corresponds to the transmembrane orientations for both P1 and P2, almost perpendicular to the plane of the bilayer (see Fig. 6) with tilt angles θ equal to 5 and 2°, respectively. The peptide depth d was 1.1 and 1.2 Å, respectively. In this situation, the tryptophan residues of P1 and P2 are located at 2.3 and 2.6 Å from the membrane centre, respectively. These values are close to the distances calculated from the parallax analysis. The small difference between the parallax and simulated position can be the result of partial unwinding of the α-helix at the peptide termini. This unwinding can allow the protein to take an energetically more appropriate position.

Hardly any difference is observed between P1 and P2, both in the spectroscopic experiments and in the polarity mismatch simulations. In the simulations, the mismatch for P1 is only 5% higher than for P2, and the most probable state is the same transmembrane configuration for both peptides. Clearly, the polarity difference between arginine and alanine makes a small difference in total mismatch for the 25 amino acid residue peptides. For the CD spectra, the tryptophan emission spectra, the acrylamide quenching experiment and the parallax analysis the differences are also negligible. This indicates a minor effect of the mutation R10A on the bilayer topology of the peptide, probably because arginine is able to position its guanido group in a more favorable position via snorkeling; this results in a lower effective polarity.

4.6. Summarizing discussion

Based on our findings, the peptides P1 and P2 adopt a transmembrane conformation, with a mainly α-helical structure in the central part, placing the tryptophan residue at position 12 at a location 4±2 Å from the centre of the lipid bilayer. For both peptides, the experimental results are in good agreement with the results obtained from polarity mismatch optimization. Consequently, the arginine at position 10 in peptide P1 is also located in the hydrocarbon core of the bilayer.

The peptides P1 and P2 are not very hydrophobic: about half of the residues are hydrophilic, the peptides contain several positively charged residues, and they dissolve readily in water. Nevertheless, the peptides appear to adopt a transmembrane configuration when vesicles are present.

For peptide P2, this intriguing behavior can be easily explained by looking carefully at the amino acid sequence. The central part of P2 is mainly hydrophobic, uncharged at neutral pH, and long enough to span a DOPC/DOPG bilayer. Favorable interactions of the flanking lysines with the negatively charged DOPG headgroups [27,52], combined with these hydrophobic interactions, promote the formation of a transmembrane helix.

Peptide P1, on the other hand, contains an arginine residue in its hydrophobic core, which normally would be positively charged at neutral pH, and its presence is expected to affect the membrane topology of the peptide. Nonetheless, no significant difference between P1 and P2 is observed. This raises questions about the behavior and protonation state of the arginine residue in P1 in a phospholipid bilayer system.

The arginine residue of peptide P1 is located at position 10, two residues further away from the centre of the bilayer as compared to the tryptophan. This would place it at approximately 7 Å from the bilayer centre, assuming an α-helical conformation. This location makes it possible for the arginine side chain to snorkel, thereby positioning its positively charged guanido group near the phospholipid headgroups. Both arginines and lysines are able to span a distance of about 6 Å with their long side chains, and can therefore, despite their

positive charge, be positioned in an α-helix five to six residues below the membrane/water interface [36]. Snorkeling effects have been invoked before to explain the positioning of charged residues in transmembrane helices in the hydrophobic core of the bilayer [15,35–38].

The fact that hardly any difference is observed between the behavior of the peptides P1 and P2 shows that the long, flexible side chain of the arginine residue in P1 is able to snorkel towards the lipid headgroup region, without altering the membrane topology of the peptide. Clearly snorkeling of the arginine is possible without causing any "stress" on the peptide backbone and other side chains. Charged residues with a shorter side chain, such as aspartic and glutamic acid, and arginines and lysines placed deeper in the hydrocarbon core of the bilayer, often promote the formation of shifted or tilted transmembrane structures, or even a non-transmembrane peptide population [15,35,36]. The arginine residue in P1 on the other hand, has a side chain long enough to reach the lipid headgroup region from its position five to six residues into the hydrocarbon core.

Apart from the essential arginine R735, helix 7 of Vph1p contains two histidine residues (H729 and H743), which are important, although not essential, for V-ATPase activity [53,54]. These histidines, located at position 4 and 18 in P1 and P2, could probably also be located in the α-helix, shown from our work to be formed in the more hydrophobic core of the peptides. His18 would be positioned at about the same depth in the lipid bilayer as the arginine, His4 is somewhat closer to the membrane–water interface. The histidines are not charged at neutral pH, but can easily pick up a proton at lower pH. Compared to arginine, the side chains of the histidines are relatively rigid [55]. The histidine residues are suggested to line the access channels leading to the carboxyl groups in Vma3p, Vma11p and Vma16p, probably via their ability to reversibly pick up protons.

Peptide P1 contains the essential arginine R735, which is proposed to interact with the glutamic acid residues in the proteolipid subunits and to force the release of protons into the luminal access channel, thereby directing unidirectional proton transport [3]. The relatively high flexibility of the arginine side chain as deduced from its snorkeling, might be a mechanism to facilitate these interactions in the V-ATPase enzyme. During proton transport, the favorable salt bridge between the positively charged arginine in Vph1p and the negatively charged glutamic acid in Vma3p, Vma11p or Vma16p has to be broken for the process to continue. The energy for breaking this bond comes from ATP hydrolysis, which results in rotation of the ring of proteolipid subunits. The fact that the long, flexible arginine side chain is able to reach towards the next glutamic acid residue directly after disturbance of interaction might facilitate this process.

Inhibitors of the V-ATPase enzyme, such as bafilomycin and concanamycin, are shown to bind to the V_0 domain, most probably to the interface between Vph1p and the ring of proteolipid subunits [8–10]. Binding of these molecules to this interface could reduce the flexibility of the essential arginine R735, thereby interfering with its interactions with the glutamic acid residues. The peptides presented in this work are excellent model systems to study these interactions of Vph1p, both with the proteolipid subunits and with V-ATPase inhibitors (Hesselink, R.W., et al., unpublished results) in further detail.

Acknowledgements

We acknowledge the European Commission for support under the Framework V, Quality of Life, initiative (QLRT-1999-31801). We thank Dr. Eefjan Breukink and Hester Hasper of the Department Biochemistry of Membranes, CBLE, IB, of Utrecht University for kindly providing the doxyl-labeled lipids used in the parallax analysis.

References

[1] M.E. Finbow, M.A. Harrison, The vacuolar H^+-ATPase: a universal proton pump of eukaryotes, Biochem. J. 324 (1997) 697–712.
[2] T. Nishi, M. Forgac, The vacuolar (H^+)-ATPases—Nature's most versatile proton pumps, Nat. Rev., Mol. Cell Biol. 3 (2002) 94–103.
[3] S. Kawasaki-Nishi, T. Nishi, M. Forgac, Proton translocation driven by ATP hydrolysis in V-ATPases, FEBS Lett. 545 (2003) 76–85.
[4] N. Nelson, W.R. Harvey, Vacuolar and plasma membrane proton-adenosinetriphosphatases, Phys. Rev. 79 (1999) 361–385.
[5] N. Dixon, T. Pali, S. Ball, M.A. Harrison, D. Marsh, J.B.C. Findlay, T.P. Kee, New biophysical probes for structure–activity analyses of vacuolar-H^+-ATPase enzymes, Org. Biomol. Chem. 1 (2003) 4361–4363.
[6] T. Murata, I. Yamato, Y. Kakinuma, A.G.W. Leslie, J.E. Walker, Structure of the rotor of the V-Type Na+-ATPase from *Enterococcus hirae*, Science 308 (2005) 654–659.
[7] S. Kawasaki-Nishi, T. Nishi, M. Forgac, Arg-735 of the 100-kDa subunit a of the yeast V-ATPase is essential for proton translocation, Proc. Natl. Acad. Sci. U. S. A. 98 (2001) 12397–12402.
[8] J. Zhang, Y. Feng, M. Forgac, Proton conduction and bafilomycin binding by the V_0 domain of the coated vesicle V-ATPase, J. Biol. Chem. 269 (1994) 23518.
[9] B.J. Bowman, E.J. Bowman, Mutations in subunit c of the vacuolar ATPase confer resistance to bafilomycin and identify a conserved antibiotic binding site, J. Biol. Chem. 277 (2002) 3965–3972.
[10] M. Huss, G. Ingenhorst, S. Konig, M. Gassel, S. Drose, A. Zeeck, K. Altendorf, H. Wieczorek, Concanamycin a, the specific inhibitor of V-ATPases, binds to the V_0 subunit c, J. Biol. Chem. 277 (2002) 40544–40548.
[11] E.J. Bowman, L.A. Graham, T.H. Stevens, B.J. Bowman, The bafilomycin/concanamycin binding site in subunit c of the V-ATPase from *Neurospora crassa and Saccharomyces cerevisiae, J. Biol. Chem. 279 (2004) 33131–33138.*
[12] T. Páli, G. Whyteside, N. Dixon, T.P. Kee, S. Ball, M.A. Harrison, J.B.C. Findlay, M.E. Finbow, D. Marsh, Interaction of inhibitors of the vacuolar H^+-ATPase with the transmembrane V_0-sector, Biochemistry 43 (2004) 12297–12305.
[13] R.H. Fillingame, W. Jiang, O.Y. Dmitriev, P.C. Jones, Structural interpretations of F_0 rotary function in the *Escherichia coli* F_1F_0 ATP synthase, Biochim. Biophys. Acta 1458 (2000) 387–403.
[14] H.E. Van Heusden, B. De Kruijff, E. Breukink, Lipid II induces a transmembrane orientation of the pore-forming peptide lantibiotic nisin, Biochemistry 41 (2002) 12171–12178.
[15] G.A. Caputo, E. London, Cumulative effects of amino acid substitutions and hydrophobic mismatch upon the transmembrane stability and conformation of hydrophobic α-helices, Biochemistry 42 (2003) 3275–3285.
[16] J.A. Killian, Synthetic peptides as models for intrinsic membrane proteins, FEBS Lett. 555 (2003) 134–138.
[17] A.S. Ladokhin, S.H. White, Interfacial folding and membrane insertion of a designed helical peptide, Biochemistry 43 (2004) 5782–5791.

[18] P.E.G. Thoren, D. Persson, E.K. Esbjorner, M. Goksor, P. Lincoln, B. Norden, Membrane binding and translocation of cell-penetrating peptides, Biochemistry 43 (2004) 3471–3489.
[19] J.-L. Popot, D.M. Engelman, Membrane protein folding and oligomerization: the two-stage model, Biochemistry 29 (1990) 4031–4037.
[20] J.-L. Popot, D.M. Engelman, Helical membrane protein folding, stability, and evolution, Annu. Rev. Biochem. 69 (2000) 881–922.
[21] M.B. Ulmschneider, D.P. Tieleman, M.S.P. Sansom, Interactions of a transmembrane helix and a membrane: comparative simulations of bacteriorhodopsin helix A, J. Phys. Chem., B 108 (2004) 10149–10159.
[22] L.P. Liu, C.M. Deber, Anionic phospholipids modulate peptide insertion into membranes, Biochemistry 36 (1997) 5476–5482.
[23] J.H. Ren, S. Lew, Z.W. Wang, E. London, Transmembrane orientation of hydrophobic α-helices is regulated both by the relationship of helix length to bilayer thickness and by the cholesterol concentration, Biochemistry 36 (1997) 10213–10220.
[24] R.J. Webb, J.M. East, R.P. Sharma, A.G. Lee, Hydrophobic mismatch and the incorporation of peptides into lipid bilayers: a possible mechanism for retention in the Golgi, Biochemistry 37 (1998) 673–679.
[25] J.H. Ren, S. Lew, J.Y. Wang, E. London, Control of the transmembrane orientation and interhelical interactions within membranes by hydrophobic helix length, Biochemistry 38 (1999) 5905–5912.
[26] J.A. Killian, G. Von Heijne, How proteins adapt to a membrane–water interface, Trends Biochem. Sci. 25 (2000) 429–434.
[27] M.R.R. De Planque, J.A. Killian, Protein–lipid interactions studied with designed transmembrane peptides: role of hydrophobic matching and interfacial anchoring, Mol. Membr. Biol. 20 (2003) 271–284.
[28] C.-N. Chin, G. Von Heijne, Charge pair interactions in a model transmembrane helix in the ER membrane, J. Mol. Biol. 303 (2000) 1–5.
[29] F.X. Zhou, M.J. Cocco, W.P. Russ, A.T. Brunger, D.M. Engelman, Interhelical hydrogen bonding drives strong interactions in membrane proteins, Nat. Struct. Biol. 7 (2000) 154–160.
[30] H. Gratkowski, J.D. Lear, W.F. DeGrado, Polar side chains drive the association of model transmembrane peptides, Proc. Natl. Acad. Sci. U. S. A. 98 (2001) 880–885.
[31] F.X. Zhou, H.J. Merianos, A.T. Brunger, D.M. Engelman, Polar residues drive association of polyleucine transmembrane helices, Proc. Natl. Acad. Sci. U. S. A. 98 (2001) 2250–2255.
[32] M. Hermansson, G. Von Heijne, Inter-helical hydrogen bond formation during membrane protein integration into the ER membrane, J. Mol. Biol. 334 (2003) 803–809.
[33] J.D. Lear, H. Gratkowski, L. Adamian, J. Liang, W.F. DeGrado, Position-dependence of stabilizing polar interactions of asparagine in transmembrane helical bundles, Biochemistry 42 (2003) 6400–6407.
[34] S. Lew, J.H. Ren, E. London, The effects of polar and/or ionizable residues in the core and flanking regions of hydrophobic helices on transmembrane conformation and oligomerization, Biochemistry 39 (2000) 9632–9640.
[35] G.A. Caputo, E. London, Position and ionization state of Asp in the core of membrane-inserted α-helices control both the equilibrium between transmembrane and nontransmembrane helix topography and transmembrane helix positioning, Biochemistry 43 (2004) 8794–8806.
[36] M. Monné, I. Nilsson, M. Johansson, N. Elmhed, G. Von Heijne, Positively and negatively charged residues have different effects on the position in the membrane of a model transmembrane helix, J. Mol. Biol. 284 (1998) 1177–1183.
[37] E. Strandberg, S. Morein, D.T.S. Rijkers, R.M.J. Liskamp, P.C.A. Van der Wel, J.A. Killian, Lipid dependence of membrane anchoring properties and snorkeling behavior of aromatic and charged residues in transmembrane peptides, Biochemistry 41 (2002) 7190–7198.
[38] E. Strandberg, J.A. Killian, Snorkeling of lysine side chains in transmembrane helices: how easy can it get? FEBS Lett. 544 (2003) 69–73.
[39] T.C.B. Vogt, B. Bechinger, The interactions of histidine-containing amphipathic helical peptide antibiotics with lipid bilayers, J. Biol. Chem. 274 (1999) 29115–29121.
[40] M.F. Manolson, D. Proteau, R.A. Preston, A. Stenbit, B.T. Roberts, M.A. Hoyt, D. Preuss, J. Mulholland, D. Botstein, E.W. Jones, The Vph1 gene encodes a 95-kDa integral membrane polypeptide required for in vivo assembly and activity of the yeast vacuolar H^+-ATPase, J. Biol. Chem. 267 (1992) 14294–14303.
[41] B. Bechinger, Membrane insertion and orientation of polyalanine peptides: a 15 N solid-state NMR spectroscopy investigation, Biophys. J. 81 (2001) 2251–2256.
[42] A.S. Ladokhin, S. Jayasinghe, S.H. White, How to measure and analyze tryptophan fluorescence in membranes properly, and why bother? Anal. Biochem. 285 (2000) 235–245.
[43] G. Buhm, CDNN: CD spectra deconvolution software version 2.1 (1997).
[44] S.C. Gill, P.H. Von Hippel, Calculation of protein extinction coefficients from amino acid sequence data, Anal. Biochem. 182 (1989) 319–326.
[45] J.R. Lakowicz, Principles of Fluorescence Spectroscopy, 2nd ed., Kluwer Academic/Plenum Publishers, New York, 1999.
[46] A. Chattopadhyay, E. London, Parallax method for direct measurement of membrane penetration depth utilizing fluorescence quenching by spin-labeled phospholipids, Biochemistry 26 (1987) 39–45.
[47] A.S. Ladokhin, in: R.A. Meyers (Ed.), Encyclopedia of Analytical Chemistry, John Wiley and Sons Ltd., Chichester, 2000, pp. 5762–5779.
[48] G.A. Caputo, E. London, Using a novel dual fluorescence quenching assay for measurement of tryptophan depth within lipid bilayers to determine hydrophobic α-helix locations within membranes, Biochemistry 42 (2003) 3265–3274.
[49] M.C. Manning, R.W. Woody, Theoretical CD studies of polypeptide helices: examination of important electronic and geometric factors, Biopolymers 31 (1991) 569–586.
[50] S.H. White, W.C. Wimley, Hydrophobic interactions of peptides with membrane interfaces, Biochim. Biophys. Acta 1376 (1998) 339–352.
[51] J.A. Nelder, R. Mead, A simplex method for function minimization, Comput. J. 7 (1965) 308–313.
[52] M.R.R. De Planque, J.A.W. Kruijtzer, R.M.J. Liskamp, D. Marsh, D.V. Greathouse, R.E. Koeppe, B. De Kruijff, J.A. Killian, Different membrane anchoring positions of tryptophan and lysine in synthetic transmembrane α-helical peptides, J. Biol. Chem. 274 (1999) 20839–20846.
[53] X.-H. Leng, M.F. Manolson, Q. Liu, M. Forgac, Site-directed mutagenesis of the 100-kDa subunit (Vph1p) of the yeast vacuolar (H^+)-ATPase, J. Biol. Chem. 271 (1996) 22487–22493.
[54] X.-H. Leng, M.F. Manolson, M. Forgac, Function of the COOH-terminal domain of Vph1p in activity and assembly of the yeast V-ATPase, J. Biol. Chem. 273 (1998) 6717–6723.
[55] T.C. Pochapsky, N.U. Jain, M. Kuti, T.A. Lyons, J. Heymont, A refined model for the solution structure of oxidized putidaredoxin, Biochemistry 38 (1999) 4681–4690.